Investigation of the Dynamic Behaviour of a Vircator, based on an Analytical Model and Experimental Observations

Panagiotis V. Betzios, Nikolaos K. Uzunoglu

Abstract— **The Virtual Cathode Oscillator (Vircator) is a high power microwave source with transient characteristics heavily dependent on the diode geometry and the pulsed power system driving the vacuum diode. A mathematical formulation can be used to predict the evolution of current, voltage and output frequency, based on the assumption of a capacitive storage element being discharged through the vircator diode. The predicted transient behavior is compared with experimental results from a side-extracted Vircator. It will be shown that this model can be used for benchmarking erratic behavior of machined cathodes.**

I. Introduction

The Virtual Cathode Oscillator is a microwave tube able to radiate short pulses of very high power microwaves, mainly in the low and middle frequency bands [1-5], The mechanisms of microwave production in Vircators are the oscillations of the virtual cathode in space and time and the oscillations of electrons trapped in the potential well between the cathode and the virtual cathode, also known as electron reflexing. These separated mechanisms of microwave radiation are also experimentally verified [2, 3, 6]. Following the well known Child-Langmuir theory [7, 8], and the analytical approach for the infinite short-circuited diode [9], a virtual cathode will be formed when an electron stream is injected in a volume, exceeding a critical current density. For the ideal short-circuited diode, the critical value for formation of a virtual cathode when injecting an electron beam, is eight-times the equivalent Child-Langmuir current limit of the polarized diode with zero emitting potential. The virtual cathode can then be retained with a four-times higher current density. On an other approach, a magnetically confined electron beam can hold a maximum current, before forming a virtual cathode in its center.

Virtual Cathode Oscillators can only operate with explosive electron emission cathodes. There is no other way to reach current densities of tens of kA/cm^2, which are needed for strong virtual cathode phenomena and powerful microwave generation. Explosive electron emission diodes suffer from a limited lifetime and from transient alteration of geometrical characteristics, due to plasma formation and expansion. Overheated cathode spots produce a metal vapor plasma that covers the cathode, and the anode follows shortly afterwards [10, 11].

Panagiotis V. Betzios and Nikolaos K. Uzunoglu are with the Microwave and Fiber Optics Laboratory, School of Electrical and Computer Engineering, National Technical University of Athens, 157 80 Athens, Greece.

Plasma expands with thermal velocity,

$$\upsilon \propto \sqrt{k_B T / m}\,, \tag{1}$$

where k_B is the Boltzmann constant, T is the plasma temperature and m is the particle mass. High electric field gradients give rise to bigger current densities, therefore higher plasma temperatures. Also electrode materials and conditioning plays an important role, since light atoms and molecules adversely affect plasma expansion speeds. Plasma expansion speeds are in the range of below 1cm/μsec up to 10cm/μsec for poorly conditioned materials and high field gradients.

II. Mathematical Formulation

Vircators are basically driven from a high voltage capacitive storage. For Marx generator driven vircators, the current flowing through the capacitor bank is the current of the vacuum diode.

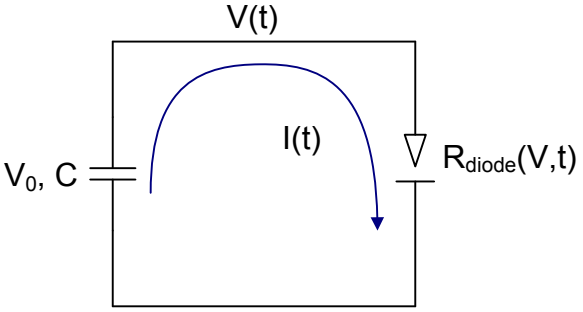

Fig. 1. Discharge of a capacitor through a vacuum diode

Diode current can be estimated by the well known Child-Langmuir formulation,

$$I_{SCL} \cong 2.33 \cdot 10^{-6} S(t) \frac{V^{3/2}(t)}{d^2(t)}. \tag{2}$$

Assuming cylindrical symmetry and homogenous plasma expansion originating from the cathode, we can write for the "active" cathode surface $S(t) \cong \pi r^2(t) \cong \pi (a + u \cdot t)^2$ and for the anode-cathode distance $d(t) \cong (d - u \cdot t)^2$. Here, a is the initial emitting cathode radius and d is the electrode separation. The current through the capacitor bank is the current of the vacuum diode, so

$$C\frac{dV}{dt} = 2.33\cdot 10^{-6}\pi\left(a+u\cdot t\right)^2 \frac{V^{3/2}}{\left(d-u\cdot t\right)^2}. \quad (3)$$

This differential equation has two real solutions, one of which is the representation of the voltage in this model. Once we solve for V, we can derive the diode current, I, using the modified 2-D Child-Langmuir law [12],

$$I_{diode} \cong 2.33\cdot 10^{-6}\pi\left(a+u\cdot t\right)^2 \frac{V^{3/2}}{\left(d-u\cdot t\right)^2}\cdot\left(1+0.26\frac{d-u\cdot t}{a+u\cdot t}\right) \quad (4)$$

Equations (3) and (4) can predict the voltage and current flowing through the cylindrically symmetric diode with circular cathode of finite radius, a, and gap spacing, d.

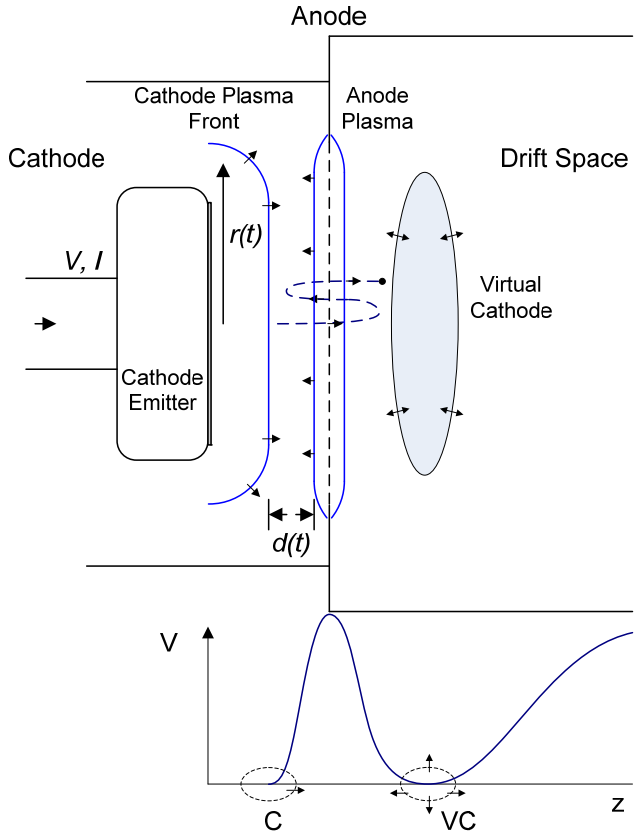

Fig. 2. Dynamic behavior of the Vircator parameters due to plasma expansion.

For the Vircator drift space, the maximum beam current, I_L, is calculated by the well known formula [13]

$$I_L \approx I_0 \frac{\left(\gamma^{2/3}-1\right)^{3/2}}{1+2\ln\left(b/a\right)}, \quad (5)$$

where γ is the Lorenz factor, a is the beam radius and b is the drift tube radius. Substituting for the Lorenz factor γ, the mesh geometrical transparency n% and assuming the beam radius to be equal to the "active" cathode radius, we can write

$$I_{diode} > 17\cdot 10^3 \frac{1}{n\%}\frac{\left[\left(1+\frac{V}{511\cdot 10^3}\right)^{2/3}-1\right]^{3/2}}{1+2\ln\left(\frac{b}{a+u\cdot t}\right)}. \quad (6)$$

This expression provides a limit for the diode current, for a virtual cathode to be formed in the drift space.

From the two mechanisms of microwave production in Vircators, the oscillations of the virtual cathode in space and time follow the plasma frequency of the electron beam, while the oscillations of electrons trapped in the potential well between the cathode and the virtual cathode can be calculated from the transit time of an electron from the cathode to the anode. The beam plasma frequency at the injection point is

$$f_{beam} = \frac{1}{2\pi}\sqrt{\frac{n_e e^2}{\varepsilon_0 \gamma m_e}}. \quad (7)$$

where n_e is the electron density, γ is the Lorenz factor and m_e is the electron rest mass. The virtual cathode oscillations follow the beam plasma frequency within the range [3, 14-16]

$$f_p \le f_{OSC} \le \sqrt{2\pi} f_p. \quad (8)$$

Woo [14] showed that the virtual cathode oscillations can be calculated from

$$f_{OSC} = \frac{4.77}{d}\ln\left(\gamma+\sqrt{\gamma^2-1}\right). \quad (9)$$

Electron reflex frequency can be derived as follows: Given the electric field E, we write for the electron acceleration

$$\frac{d}{dt}\left(\frac{m\upsilon}{\sqrt{1-\upsilon^2/c^2}}\right) = eE. \quad (10)$$

Integrating for zero initial velocity and solving for υ, we get

$$\upsilon(t) = \pm\frac{eEt}{m\sqrt{1+\left(\frac{eE}{mc}\right)^2 t^2}}. \quad (11)$$

Thus, we solve for the distance traveled,

$$x(t) = \pm\int_0^t \frac{\mu}{\sqrt{1+\frac{\mu^2}{c^2}\xi^2}}\xi d\xi, \quad (12)$$

with $\mu = eE/m$. This integral yields

$$x(t) = \pm\frac{c^2}{\mu}\left[\sqrt{1+\left(\frac{\mu t}{c}\right)^2}-1\right]. \quad (13)$$

Supposing that $E = V/d$ in the diode region, we solve for t, so that the transit time from the cathode to the anode is

$$\tau_{AK} = \frac{d}{\sqrt{V}}\sqrt{\frac{2m}{e}+\frac{V}{c^2}} \quad (14)$$

Consequently, the reflex frequency can be approximated by

$$f_{REFL} = \frac{1}{4\tau_{AK}} = \frac{\sqrt{V}}{4d}\sqrt{\frac{ec^2}{2mc^2 + eV}}, \quad (15)$$

under the assumption that the real and the virtual cathode are equidistant from the anode. It can be seen that these radiation mechanisms heavily depend on the electron beam energy or, equivalently, on the diode voltage, V, and on the anode-cathode spacing, d. The reflex oscillations produce a microwave output proportional to $V^{1/2}$, and inversely proportional to d,

$$f_{REFL} \propto \frac{\sqrt{V_{AK}}}{d}, \quad (16)$$

an observation that is widely experimentally observed [1, 15, 17]. Also, since the beam plasma frequency is a function of the energy and the electron density, this quantity follows the Vircator diode current emission laws, which is the well known Child-Langmuir formulation, for a given diode voltage, V, and on the anode-cathode spacing, d. Therefore, the plasma frequency is also bound to the diode voltage and the anode-cathode spacing, thus making both microwave production mechanisms dependent on the same scaling law.

III. Comparison with Experiment

The Vircator used in the experiments is a *vertical* or *side* extraction type [4, 5, 18, 19], constructed on a WR430 rectangular waveguide. Various cathodes are used. One of them is a stainless steel pin, spaced 15mm away from the stainless steel anode mesh. The Vircator is maintained at high vacuum with a 100lt/s ion pump. Outgassing and leaks limit the attainable, within a reasonable time, vacuum inside the vircator in the order of 10^{-5}Torr. The Vircator can be left unpumped, and continuous operation will quickly rise the tube pressure to 10^{-3} Torr. For the experimental tests, the vircator is continuously evacuated by the ion pump.

The high voltage setup for driving the Vircator is comprised by a VDE-b impulse waveform setup, with a 140kV, 6nF charging capacitor and a 1.2nF, 140kV capacitive divider. The test voltage is a non-standard 0.5/50 waveform. Given the capacitance of the divider, and neglecting the capacitance of the tube itself, the voltage waveform rises to an approximate 80% of the impulse voltage, due to charge sharing. The vircator was driven with this configuration, and the voltage, current and microwave signals were stored on an Agilent DSO80204A digitizing oscilloscope. The diode voltage was recorded from the capacitive divider with a Schaffner MD-200 100:1 voltage probe, the tube current was measured on the vircator ground return with a Pearson 1025 model current transformer and the microwave signal was measured with a small electric field probe placed inside the waveguide.

With a ~110kV driving impulse waveform, the currents measured were in the order of 2kA and microwave signals in the order of few kW in the 1.4GHz to 2.2GHz range.

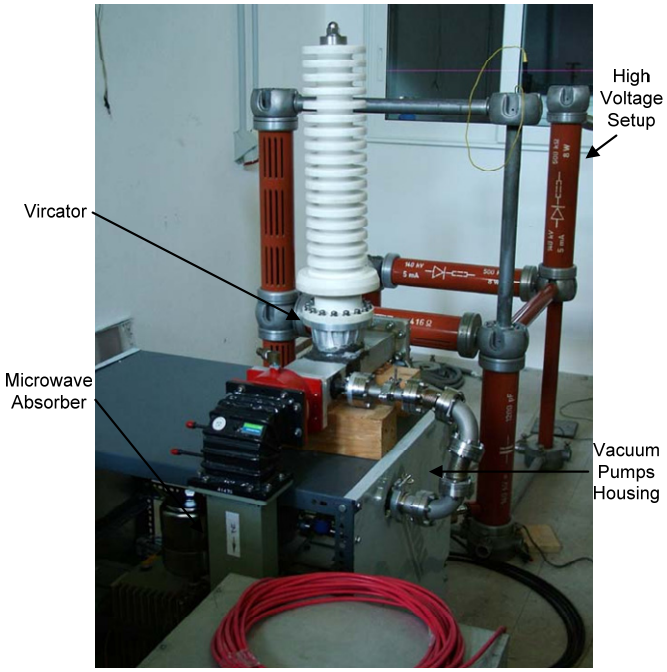

Fig. 3. Vertical extraction Vircator experimental setup.

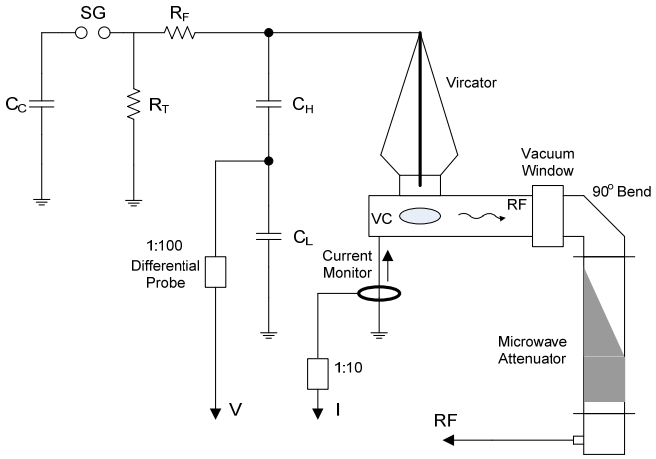

Fig. 4. Experimental setup with vertical extraction vircator and VDE-b impulse waveform test system.

The experimental configuration described below is a diode with a stainless steel pin, spaced 15mm away from the anode. The anode is a stainless steel mesh of 75% geometric transparency, woven from of 0.3mm thick wires. One parameter that is not a-priori known is the plasma expansion frequency. Initial measurements have shown that this configuration collapses at 300nsec, yielding a 5cm/μsec plasma expansion rate. This relatively high plasma expansion speed is attributed to high concentrations of hydrogen and water, that are usually absorbed in stainless steels. Using the differential equation (3) we can calculate the transient behavior of the diode voltage, for a given initial value applied to the diode. Then, the diode flowing through the diode can be estimated from (4). The pulsed power delivered to the tube can be calculated by multiplying these two metrics. Equation (5) yields the needed beam current, in order to form a virtual cathode inside the drift tube,

provided the beam energy, drift tube diameter and mesh transparency. The drift tube diameter is set to the rectangular waveguide big dimension, namely 109.2mm fro the WR430 type. The modeled behavior can be depicted as follows:

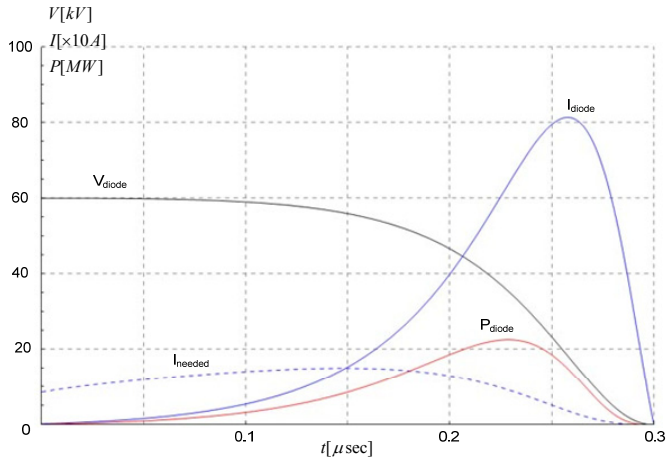

Fig. 5. Transient behavior of the vircator diode, for given initial voltage, plasma expansion rates and capacity of the energy storage element.

Once the voltage and current parameters are calculated, the estimations of the output frequencies can be plotted. In the following diagram we include the beam plasma frequency, (7), the expected region of virtual cathode oscillations, (8), the Woo estimation of the oscillation frequency, (9) and the reflex frequency estimation (15), both the relativistic (15) and the non-relativistic, yielded by ignoring the energy term eV inside the square root quantity.

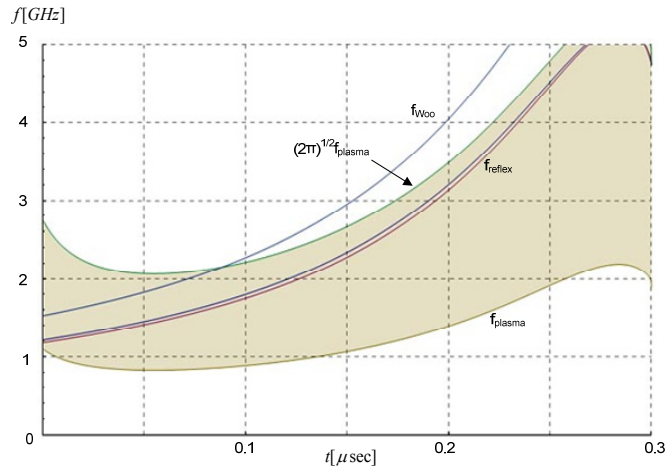

Fig. 6. Transient behavior of the vircator frequencies, for given initial voltage, plasma expansion rates and capacity of the energy storage element.

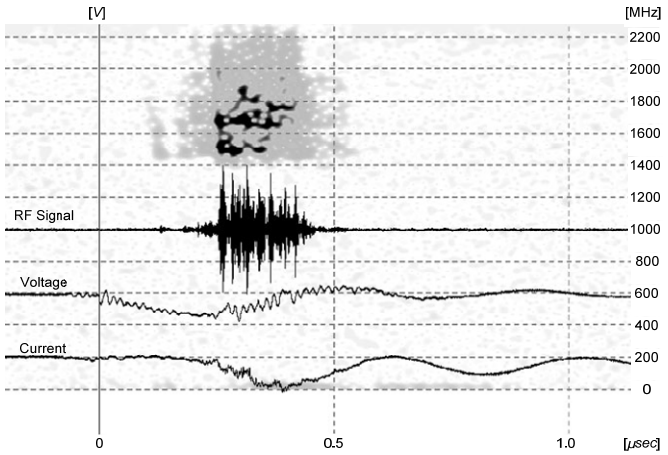

Fig. 7. Measured voltage, current and high frequency output of the vertical extraction vircator. A time-frequency graph is included, showing frequency content of the signal. Cutoff of the waveguide is 1380MHz. Peak voltage is 62kV, peak current is 860A. Microwave signal is about one kW.

The diode of the Vircator is primarily fed by the capacitive voltage divider, a 1.2nF, 140kV capacitor. The power delivered to the diode is backed by the prime charging capacitor C_C, a 140kV, 6nF element. The beginning of the diode collapse is estimated at the point where voltage reaches its maximum and current through the vircator begins to flow. Due to the existence of the charging capacitor C_C, the current waveform has somehow higher than predicted amplitude and longer duration. The important thing is that the experimental results well agree with the waveforms and frequency content that the model predicts.

IV. Conclusion

A model for designing the vircator operation is demonstrated herein. The significance of the analytical approach is that it predicts the dynamic behavior of a vircator, being driven by a high voltage capacitive storage. Since vircators are usually pulsed from Marx generators, the model can accurately give the designer an insight on the capacitance needed, the diode dimensions and the frequency output of the tube. These predictions well agree with the metrics of a low voltage vertical extraction vircator that has been constructed and tested. By using the model as a benchmark, we can reverse engineer a cathode that may not operate as designed. The approach can be fitted to measured currents, voltages and gap closure rates, to examine the “active” area of electron emission from cylindrical cathodes that may not emit electrons from their whole surface, or from velvet cloth cathodes that may have sustained a damage and present localized favorable emission sites.

REFERENCES

[1] R. A. Mahaffey, P. Sprangle, J. Golden, and C. A. Kapetanakos, "High-Power Microwaves from a Nonisochronic Reflecting Electron System," Phys. Rev. Lett., vol. 39, no. 13, pp. 843-846 1977.

[2] S. C. Burkhart, R. D. Scarpetti, and R. L. Lundberg, "A virtual-cathode reflex triode for high-power microwave generation," J. Appl. Phys., vol. 58, no. 1, pp. 28-36, 1985.

[3] H. A. Davis, R. R. Bartsch, L. E. Thode, E. G. Sherwood, and R. M. Stringfield, "High-Power Microwave Generation from a Virtual Cathode Device," Phys. Rev. Lett., vol. 55, no. 21, pp. 2293-2296 1985.

[4] J. Benford, H. Sze, W. Woo, and B. Harteneck, "Virtual-cathode oscillator emission by a pinched diode," Phys. Rev. Lett., vol. 56, no. 4, pp. 344-346, 1986.

[5] H. Sze, J. Benford, W. Woo, and B. Harteneck, "Dynamics of a virtual cathode oscillator driven by a pinched diode," Phys. Fluids, vol. 29, no. 11, pp. 3873-3880, 1986.

[6] M. Haworth, R. Adler, B. Anderson, M. Connaughton, W. Dungan, J. Enns, J. Metz, P. Pelletier, R. Platt, J. Polaco, R. Rupp, L. Thode, and D. Voss, "Experimental observation of two microwave radiation mechanisms with widely separated frequencies during the output pulse of a high-voltage virtual cathode oscillator," Appl. Phys. Lett., vol. 59, no. 4, pp. 408-410, 1991.

[7] C. D. Child, "Discharge from Hot CaO," Phys. Rev., vol. 32, no. 5, pp. 492-511, 1911.

[8] I. Langmuir, "The Effect of Space Charge and Residual Gases on Thermionic Currents in High Vacuum," Phys. Rev., vol. 2, no. 6, pp. 450-486, 1913.

[9] C. K. Birdsall and W. B. Bridges, Electron Dynamics of Diode Regions: Academic Press Inc., 1966.

[10] I. D. Chalmers and B. D. Phukan, "Photographic Observations of Impulse Breakdown in Short Vacuum Gaps," J. Phys. D: Appl. Phys., vol. 12, pp. 1285-1292, 1979.

[11] R. Gomer, Field Emission and Field Ionization (AVS Classics of Vacuum Science and Technology): Springer, 1993.

[12] Y. Li, F. He, C. Liu, and J. Sun, "Two-Dimensional Child-Langmuir Law for Planar Diode with Finite-Radius Emitter," 5th Int. Conf. on Vacuum Electron Sources (IVESC 2004). Proceedings, pp. 263-264, 2004.

[13] L. S. Bogdankevich and A. A. Rukhadze, "Stability of Relativistic Electron Beams in a Plasma and the Problem of Critical Currents," Sov. Phys. Usp., vol. 14, no. 2, 1971.

[14] W.-Y. Woo, "Two-dimensional Features of Virtual Cathode and Microwave Emission," Phys. Fluids, vol. 30, no. 1, pp. 239-244, 1987.

[15] D. J. Sullivan, "High Power Microwave Generation from a Virtual Cathode Oscillator (Vircator)," IEEE Trans. Nucl. Sci., vol. 30, no. 7, pp. 3426-3428, 1983.

[16] H. A. Davis, R. R. Bartsch, T. J. T. Kwan, E. G. Sherwood, and R. M. Stringfield, "Experimental confirmation of the reditron concept," IEEE Trans. Plasma Sci., vol. 16, no. 2, pp. 192-198, 1988.

[17] D. Price, D. Fittinghoff, J. Benford, H. Sze, and W. Woo, "Operational Features and Microwave Characteristics of the Vircator II Experiment," IEEE Trans. Plasma Sci., vol. 16, no. 2, pp. 177-184, 1988.

[18] C. S. Hwang, M. W. Wu, P. S. Song, and W. S. Hou, "High power microwave generation from a tunable radially extracted vircator," J. Appl. Phys., vol. 69, no. 3, pp. 1247-1252, 1991.

[19] C. S. Hwang and M. W. Wu, "A High Power Microwave Vircator with an Enhanced Efficiency," IEEE Trans. Plasma Sci., vol. 21, no.2, pp. 239-242, 1993.